

Bayesian Hierarchical Factor Regression Models to Infer Cause of Death From Verbal Autopsy Data

Kelly R. Moran¹, Elizabeth L. Turner¹, David Dunson¹, and Amy H. Herring¹

¹Duke University, Durham, USA

Abstract

In low-resource settings where vital registration of death is not routine it is often of critical interest to determine and study the cause of death (COD) for individuals and the cause-specific mortality fraction (CSMF) for populations. Post-mortem autopsies, considered the gold standard for COD assignment, are often difficult or impossible to implement due to deaths occurring outside the hospital, expense, and/or cultural norms. For this reason, Verbal Autopsies (VAs) are commonly conducted, consisting of a questionnaire administered to next of kin recording demographic information, known medical conditions, symptoms, and other factors for the decedent. This article proposes a novel class of hierarchical factor regression models that avoid restrictive assumptions of standard methods, allow both the mean and covariance to vary with COD category, and can include covariate information on the decedent, region, or events surrounding death. Taking a Bayesian approach to inference, this work develops an MCMC algorithm and validates the Factor Regression for Verbal Autopsy (FARVA) model in simulation experiments. An application of FARVA to real VA data shows improved goodness-of-fit and better predictive performance in inferring COD and CSMF over competing methods. Code and a user manual are made available at <https://github.com/kelrenmor/farva>.

Keywords: Cause of death, Covariance regression, Factor analysis, Semi-supervised classification, Verbal autopsy

1 Introduction

When it comes to the global burden of disease, the weight falls most heavily on the shoulders of low-income countries. As measured by Disability Adjusted Life Years (DALYs) lost, estimated global rates range from 40,000 to 70,000 DALYs per 100,000 individuals across low-income countries. On the other hand, rates in most developed countries tend to fall between 10,000 and 30,000 DALYs per 100,000 individuals [Global Burden of Disease Collaborative Network, 2017, Roser and Ritchie, 2018]. Furthermore, many deaths in low-income countries occur without registration, recording, or notice by the health system [Nichols et al., 2018]. Hospitals, community health workers, and public health planners are hindered in their ability to treat new patients, allocate resources, and plan for the future when the landscape of cause of death (COD) is poorly mapped.

Medical certification of cause of death without an autopsy is difficult in most cases. Unfortunately, performing an autopsy is often infeasible or impossible. Decedents often pass away in the home. If deaths occur in the hospital, the next of kin may not agree to a full or even minimally invasive autopsy. If the next of kin does agree, the hospital may lack the resources to perform the autopsy, or the findings may be inconclusive. In cases where no medical certification occurs, verbal autopsy (VA) offers a practical alternative approach for assessing cause of death. VA involves exploring the signs and symptoms (hereafter referred to only by symptoms) a decedent experienced before death by structured interview with a relative or caregiver of the deceased. Questions can include details such as “For how long was [decedent name] ill before they died?” and “Did [decedent name] have a fever in the three weeks leading up to death?” The 2016 World Health Organization (WHO) VA instrument [Gen, 2017], available online at <https://www.who.int/healthinfo/statistics/verbalautopsystandards/en/>, offers a standardized form by which VA data may be recorded.

One option for analyzing these VA records is to have physicians go through and decide on a COD for each decedent. However, this process is time consuming and takes resources away from existing patients in already resource-limited settings. In addition, such expert labeling may differ when multiple physicians are presented with the same data. An alternative approach is computer-coded VA, in which the COD is assigned via an algorithm or probabilistic model.

Existing computer-coded VA algorithms include those for which the relationship between symptoms and cause of death is encoded by experts (InterVA [Byass et al., 2012] and InSilicoVA [McCormick et al., 2016]) and those for which it is learned by relying on a labeled subset of the data having known COD (the King and Lu method [King et al., 2008], the Tariff method [James et al., 2011], the Simplified Symptom Pattern method [Murray et al., 2011a], the naive Bayes classifier [Miasnikof et al., 2015], the Bayesian factor model [Kunihama et al., 2018], and latent Gaussian graphical model [Li et al., 2018b]).

The majority of the work on VA algorithms relies on a conditional independence assumption [McCormick et al., 2016, Byass et al., 2012, James et al., 2011, Miasnikof et al., 2015]. That is, assume that once the cause of death is known, the knowledge that an individual had symptom A should not impact belief that an individual had symptom B for ANY combination of symptoms A and B . Recent work [Li et al., 2018b, Kunihama et al., 2018] has shown that this assumption is not valid in general. Logically, this finding is unsurprising; for example, the knowledge that someone had difficulty breathing would increase belief that they had a cough even given that their COD is already known.

Li et al. [2018b] and Kunihama et al. [2018] have relaxed the conditional independence assumption by probabilistically addressing conditional associations of symptoms given causes. The Bayesian latent Gaussian graphical model of Li et al. [2018b] assumes the conditional dependence structure is common across causes, i.e., the symptom-level correlation does not vary with cause. On the other hand, the latent factor model of Kunihama et al. [2018] models the symptom-level association independently for each cause. Neither allows for covariates (e.g. age, season, malaria endemicity of region) to be included in the model unless they are treated as “symptoms” themselves. The capability to allow covariates to affect cause assignment is potentially quite useful. For example, the information that an individual had balance and memory issues may be highly informative for certain CODs given an individual is young, but be uninformative among elder decedents for whom such symptoms are quite common.

The Population Health Metrics Research Consortium (PHMRC) created an open source “Gold Standard” VA database for training and testing VA models [Murray et al., 2011b]. This database uses a standardized VA questionnaire developed by the PHMRC based on WHO standards. These data include 7,840 “adults” (defined by both the WHO and PHMRC questionnaires to

mean decedents aged 12 and older), 2,075 children (1 month to 11 years old), 1,629 neonates (less than 1 month old), and 1,002 stillbirths (born deceased). Potential causes for analysis number 34 for adults (see Figure 1), 21 for children, and 10 for neonates. Locations include six sites

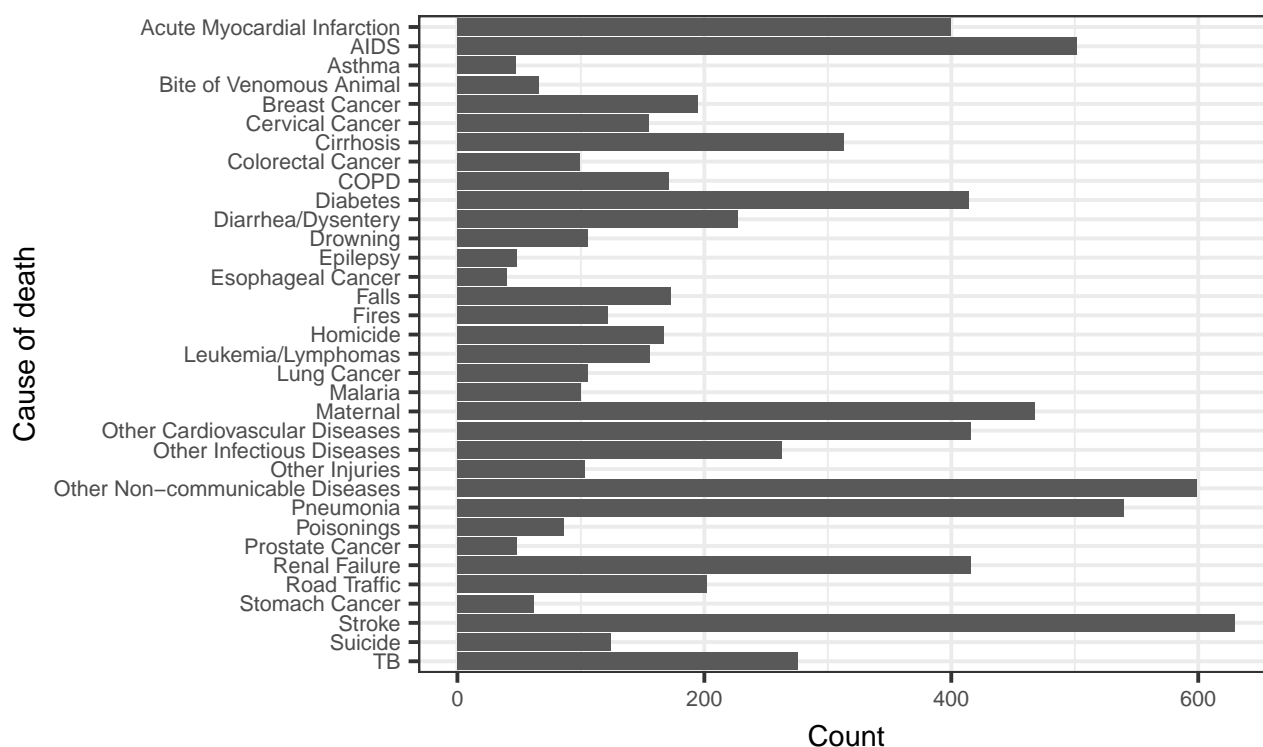


Figure 1: Number of deaths due to each of the 34 broad cause groupings in the adult PHMRC data set ($n = 7840$). See the online supplementary materials for an analogous plot broken down by age.

across four countries, and data were collected from 2007-2010. The ensuing examination of the PHMRC data illustrates the importance of allowing both the mean and the covariance to vary with both COD and covariate information, highlighting the importance of the methodological development in this article.

Figures 2 and 3 offer illustrative data-driven examples from the adult PHMRC data set using the five symptoms of fever, cough, chest pain, weight loss, and headaches and the three broad COD clusters AIDS/TB, cardiovascular conditions (including heart attack and other cardiovascular diseases), and injuries (including road traffic, drowning, falls, fires, homicides, suicides, and other injuries). These COD clusters encompass 11 of the 34 PHMRC-defined COD categories. Figure 2 shows that the prevalence of symptoms varies significantly with age. For example, across all causes (seen in the bottom row of the figure) the prevalence of the interviewee reporting the decedent experienced weight loss increases with decedent age. However, for AIDS/TB deaths the prevalence of reported weight loss remains relatively stable across ages, and is much higher

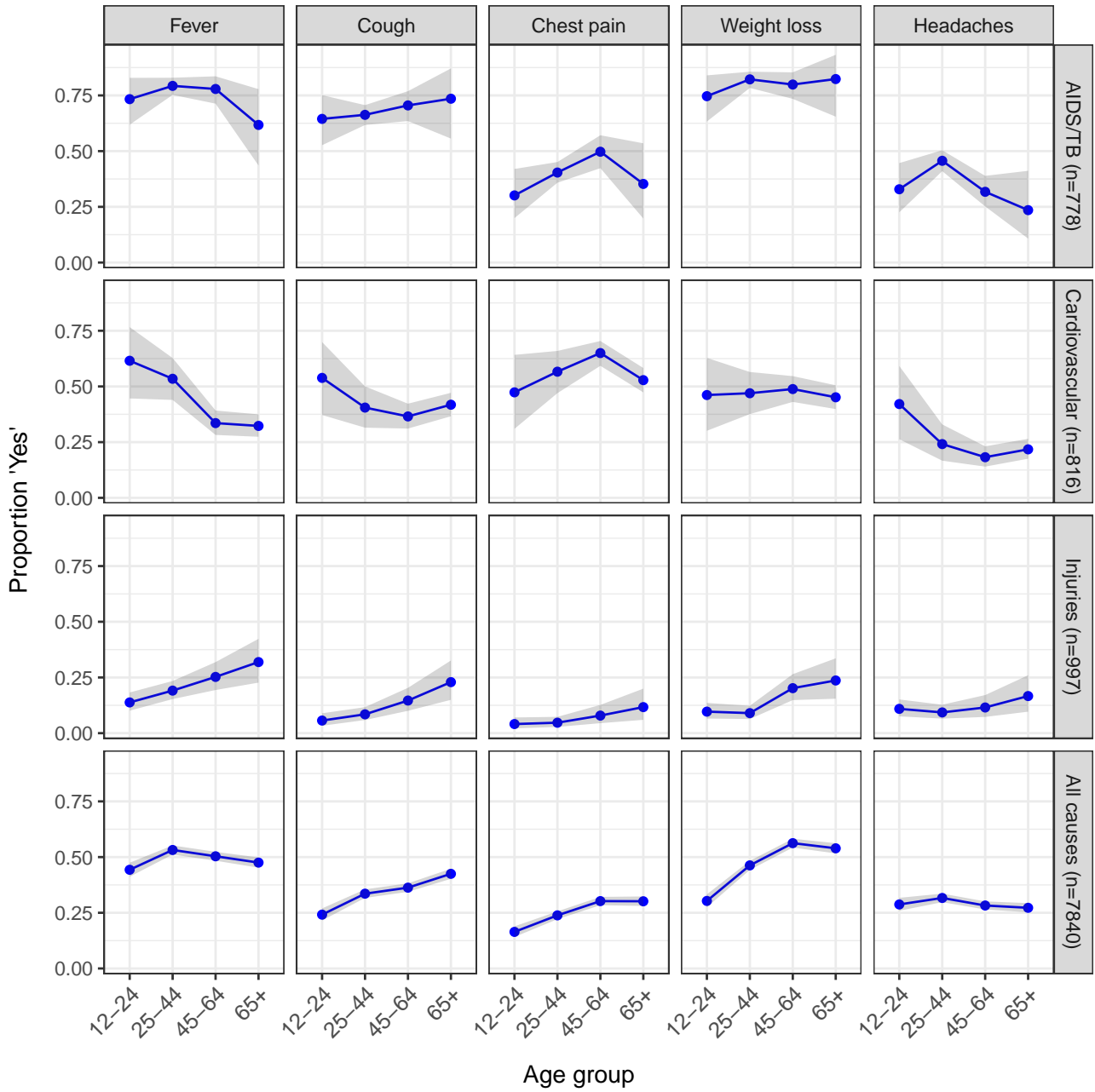


Figure 2: The average proportion of symptoms present varies across both age and cause of death (COD) in the adult PHMRC data. Each subplot corresponds to the proportion of “Yes” responses given by interviewees when asked about each symptom. Rows correspond to COD groups and columns correspond to symptoms. Proportion point estimates (points) and 95% confidence intervals (bands) are calculated by binning the binary responses by age group and calculating the frequentist estimated proportion of ‘yes’ responses for each symptom/cause combination. Responses of don’t know or refuse to answer are omitted from both the numerator and denominator of the mean and confidence interval calculations. Age was unknown for 123 individuals, who are omitted from age-specific subplots. A more detailed figure showing the number of observations contributing to each data point is provided in the online supplementary materials.

than in the full population. Estimates are more precise for CODs having more observations.

Figure 3 illustrates that the association between the set of example symptoms varies with both age group and COD. Across all CODs (seen in the bottom row of the figure), the association

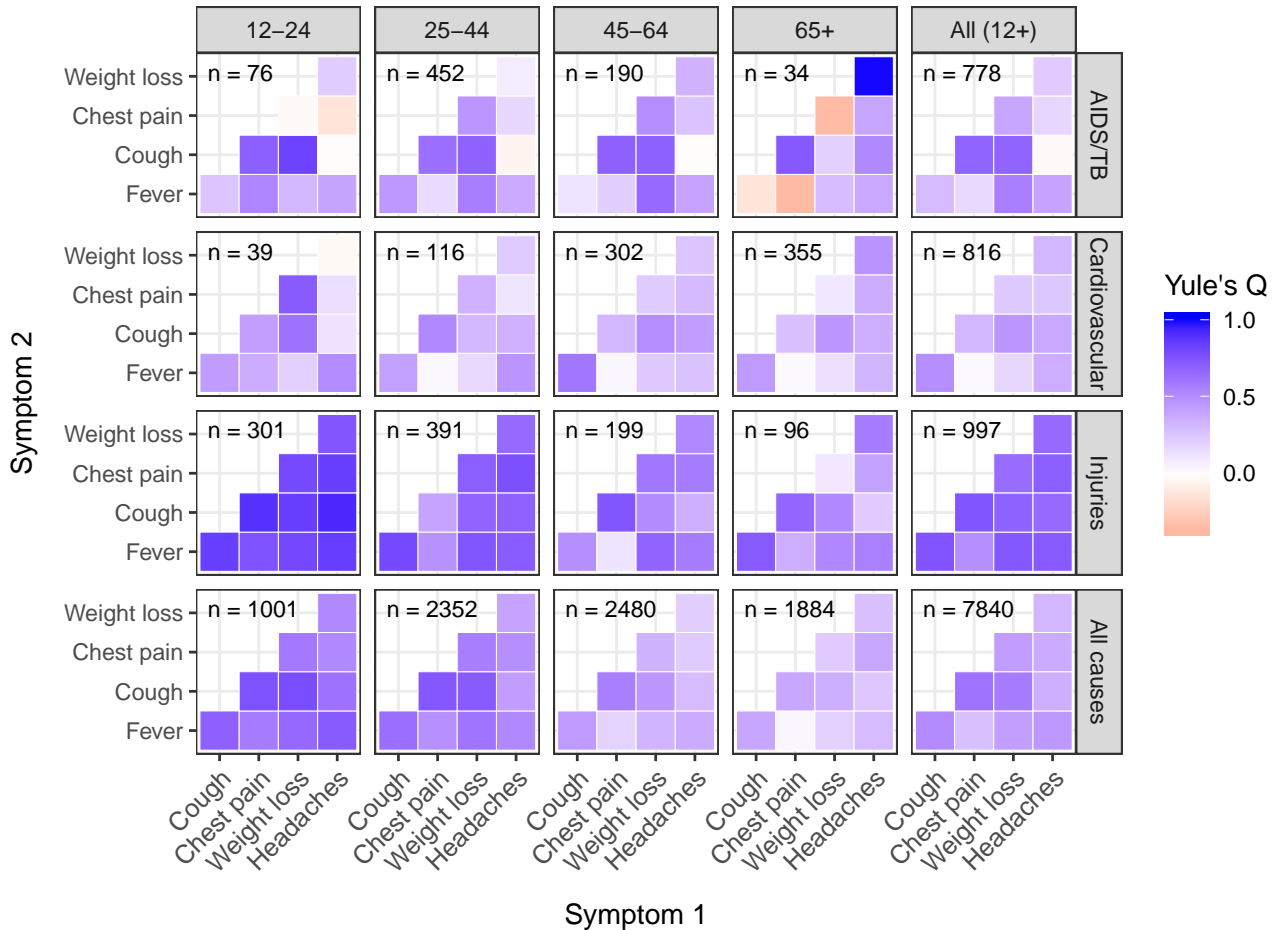


Figure 3: The association between symptoms varies across both age and cause of death (COD). Each subplot corresponds to the association between pairs of select symptoms in the adult PHMRC data as measured by Yule's Q (possible range -1 to 1). Rows correspond to COD groups and columns correspond to age groups. "Don't know" or "refused to answer" responses were omitted for the Yule's Q calculations. Sample sizes for each combination of COD/age group (i.e. the number of possible observations within that square) are shown in the top left of the subplots. Age was unknown for 123 individuals, who are omitted from age-specific subplots. For a given row, the discrepancy between the final column total and the sum of the first four columns is due to the number of missing age values for decedents having one of those CODs. A more detailed figure showing the number of observations contributing to the calculations in each subplot symptom-by-symptom square is provided in the online supplementary materials.

between symptoms weakens with age. Using an extension of McNemar's test [Zhao et al., 2014], the null hypothesis of homogeneous age group effects is rejected at the 0.05 level for all 10 of these illustrative symptom pairs (and for 72% of the 14432 testable symptom pairs in the data set, i.e. those pairs of symptoms for which at least two of the category-level 2×2 tables

have all nonzero margins— results not shown, but code available in the online supplementary materials). This finding could be due to the fact that older people tend to have more ailments in general (imagine asking a grandmother about her everyday symptoms), while younger people likely experience clusters of symptoms relating to a specific illness. Across all ages (seen in the far right column of the figure), there are differences in associations between symptoms by cause. Again using the test of Zhao et al. [2014], the null hypothesis of homogeneous COD effects is rejected at the 0.05 level for all 10 of these illustrative symptom pairs (and for 88% of all 14065 testable pairs in the data set). In summary, the data presented in Figures 2 and 3 show that both symptom prevalence and pairwise association vary by decedent age.

To the authors’ knowledge, no existing methods consider potential covariate impacts on the prevalence or association of symptoms. Furthermore, few move beyond the conditional independence assumption (that is, that the probability of observing symptom are independent given COD). Only two current works explicitly model the conditional covariance between symptoms: Li et al. [2018b] and Kuniyama et al. [2018]. The former models one common covariance structure across causes, while the latter models cause-specific symptom-level association via a latent factor model. The FActor Regression for Verbal Autopsy (FARVA) model described in the current paper has the most in common with Kuniyama et al. [2018], which also models symptom-level association via a latent factor model. FARVA extends Kuniyama et al. [2018] in several key ways. It defines both the mean and the covariance of the latent variable associated with the symptom vector hierarchically so as to share information while still allowing flexibility across disparate causes. Furthermore, it allows the mean occurrence of symptoms and covariance between symptoms to depend on individual-level covariates (e.g., age). Section 2.1 discusses existing methods and distinct advantages of FARVA relative to the model of Kuniyama et al. [2018]. Sections 2.2 and 2.3 describe the FARVA model and sampler. Section 2.4 describes a simulation experiment designed to separate aspects of performance of existing VA algorithms, and the model testing performed using real data. Section 3 reports performance of select methods using simulated and PHMRC data with regard to CSMF accuracy, top cause assignment accuracy, and the chance-corrected concordance metric proposed by Murray et al. [2014]. Section 4 discusses future directions for this model and for the field of probabilistic COD assignment using VA data.

2 Model

Let $y_i \in \{1, \dots, C\}$ denote the underlying cause of death of person $i, i = 1, \dots, N$ and $\mathbf{s}_i = (s_{i1}, \dots, s_{iP})'$ be a vector of symptoms as measured by a verbal autopsy instrument. Consider the model:

$$\pi(y_i = c | \mathbf{s}_i) = \frac{\pi(\mathbf{s}_i | y_i = c)\pi(y_i = c)}{\sum_{c^*=1}^C \pi(\mathbf{s}_i | y_i = c^*)\pi(y_i = c^*)}. \quad (1)$$

Here the probability that the COD of person i equals c is modeled conditional on the reported symptoms. The predictive goal of the model is to infer COD in cases where only symptoms are observed and the true cause is unknown. Using the above model, one can also calculate the posterior cause specific mortality fraction (CSMF, the population proportion of deaths attributed to each cause; see equation (A.2) in the Appendix) for the population of interest. The modeling choices remaining to be made are in how to treat the prior distribution over causes $\pi(y_i)$ and how to model the likelihood of symptoms given causes $\pi(\mathbf{s}_i | y_i)$.

2.1 Previous work

Often in regions in which VA methods are adopted, there is little knowledge about the population CSMF. Even in cases where clinical cases in the living are studied, causes of disease are difficult to pin down [Crump et al., 2013]. Furthermore, it is not necessarily known which diseases are most contributory to deaths, especially outside of the hospital setting. Thus the major distinguishing feature in the existing body of work on VA algorithms is in the treatment of $\pi(\mathbf{s}_i | y_i)$, rather than that of $\pi(y_i)$.

Three commonly cited non-probabilistic methods are the Tariff method [James et al., 2011], the King-Lu (KL) method [King et al., 2008], and the Simplified Symptom Pattern (SSP) method [Murray et al., 2011a]. The Tariff method is a score-based system that uses a heuristic (that tends to do well) rather than a probabilistic formulation. Tariff gives a score to each combination of cause and symptom. These scores are used to assign a value to each possible death-cause combination, and this value is then used to rank CODs for each individual. An improved version of the Tariff method [Serina et al., 2015] is the foundation for the SmartVA-Analyze Application, available at <http://www.healthdata.org/verbal-autopsy/tools>. The KL method is

designed to only estimate the CSMF and uses the assumption that the probability of symptoms given causes is the same in both the set of data for which COD is known (usually referred to as the training set) and that for which COD is unknown; it cannot infer individual cause of deaths (CODs). The closer this assumption is to the truth, and the more training data are available, the better this method will do. The SSP method uses the CSMF calculated from the KL method and calculates individual CODs using averages for the probability of symptoms given causes calculated across multiple random draws of symptoms. In each non-probabilistic method, some set of decedents having known COD are required for the model to learn a mapping between patterns of symptoms and COD.

InterVA was the first VA model to frame the relationship between symptoms and causes in a more probabilistic light [Byass et al., 2012]. Rather than relying on some training data for which COD is known, InterVA relies on a matrix of physician-generated scores assigned to the probability of observing each symptom given each cause (denoted by the $P(s|c)$ matrix, referring to the probability of symptom s given cause c). For example, physicians were asked to rate the probability that someone would answer “Yes” to “Did the patient have a cough” given that they died of TB, stroke, a motorcycle accident, etc. This matrix is useful because it allows models to be run in settings in which no training data are available. It is problematic because the values in this $P(s|c)$ matrix are likely not generalizable to all settings, are difficult to elicit (much of physician experience is likely in clinical cases and not deaths, and often the cause is not known), or may be internally inconsistent (because there are so many entries to fill out, it is very easy to, e.g., rank the probability of a patient having a cough for at least a month as higher than the probability of the patient having a cough for at least a week, even though the former case is a subset of the latter). InterVA models the probability of symptoms given causes as conditionally independent for all symptoms and causes.

There are three main issues with InterVA. First, the score used by InterVA to assign causes is based only on the presence of symptoms; it disregards symptoms when they are absent. Second, it is not possible to quantify uncertainty because the model does not contain features that are allowed to vary probabilistically. Third, InterVA is unable to incorporate physician-coded VA cases (i.e., gold standard data) into its algorithm. InSilicoVA (McCormick, 2016) is an extension of InterVA in both name and spirit. It addresses the three main issues with InterVA and provides

a valid probabilistic framework in which the main ideas of InterVA can live. That is, InSilicoVA returns valid uncertainty estimates for both the COD and CSMF values. However, it still relies on the conditional independence assumption of InterVA. An even simpler framing for VA modeling directly uses a naive Bayes classifier (NBC) to assign the probability of a death being due to a given cause for each individual and each cause [Miasnikof et al., 2015]; the COD with the highest probability is then treated as the cause. Again, this framing relies on the conditional independence assumption.

Two more recent models that have relaxed the conditional independence assumption are the latent Gaussian graphical model of Li et al. [2018b] and the factor model of Kuniyama et al. [2018]. Both models allow the prevalence of symptoms to vary by cause. The model of Li et al. [2018b] assumes a shared covariance matrix between symptoms across all causes. On the other hand, the model of Kuniyama et al. [2018] defines separate covariance matrices for each cause. The former has the advantage of allowing for mixed data (i.e., not just binary indicators), but neither model allows for demographic, spatial, or temporal information to inform the prevalence of symptoms nor their covariance.

2.2 Proposed model

FARVA is a probabilistic model for VA data in which some decedents have known COD (i.e., there exists some labeled training data) and there is interest in learning about individual COD, population CSMF, and/or the mean and covariance structure of responses in the symptom questionnaire. The explicit goals of the FARVA model proposed here are to:

- Capture dependence of symptoms given a cause.
- Share information across causes via hierarchical modeling to improve estimates associated with causes having few observed deaths.
- Allow both the conditional prevalence and the conditional association between symptoms to vary with covariates (e.g., age of patient, time of year, geographic region).
- Probabilistically predict cause of death for a new individual given their symptoms.
- Improve on COD and CSMF estimation relative to current state-of-the-art VA algorithms.

2.2.1 Prior over causes

Using a Bayesian approach to characterize uncertainty in the proportions of deaths in each COD category, let:

$$\{\Pr(y_i = 1), \dots, \Pr(y_i = C)\} \sim \text{Dirichlet}(a_1, \dots, a_C). \quad (2)$$

Under the assumption that little is known about the CSMF in the region of interest and the number of possible causes is high relative to the number of common causes, set $a_1 = \dots = a_C < 1$. This choice leads to equal probability of each cause a priori (i.e., $\pi(y_i = c) \propto 1 \forall c \in \{1, \dots, C\}$ where $\pi(y_i)$ is a probability distribution over causes of death) and encourages concentration near sparse subvectors. This assumption is likely valid in real applications; e.g., the gold standard PHMRC data set exhibits many causes having few observed deaths (see Figure 1). However, this prior can easily be modified to incorporate prior knowledge about the CSMF or to encourage uniformity in the CSMF. For example, if a pilot study performed in the region of interest found counts n_c attributable to COD $c, c = 1 \dots C$, then an option for an informed prior is $a_1 = n_1, \dots = a_C = n_C$. If uniformity was desired, one could set $a_1 = \dots = a_C = 1$.

2.2.2 Likelihood of symptoms given a cause

Recall that the likelihood takes the form $\pi(\mathbf{s}_i|y_i)$, i.e. we want to model the distribution of the symptom vector \mathbf{s}_i conditional on COD y_i . Throughout the likelihood description, the motivation behind each modeling decision and a short description of said decision will be stated in bold preceding each mathematical description.

Motivation: Symptom data includes questions on duration of symptoms in addition to their presence/absence. Therefore, allow the model to encompass data of mixed type. In order to allow the FARVA model to encompass data of binary, continuous, count, and categorical type, in the specification of $\pi(\mathbf{s}_i|y_i)$ define:

$$s_{ij} = f_j(z_{ij}), \quad j = 1, \dots, P, \quad (3)$$

where $\mathbf{z}_i = (z_{i,1}, \dots, z_{i,P})'$ is a vector of latent continuous symptoms. The particular link function f_j depends on the symptom specification, allowing for mixed scale data via selection of an

appropriate link by scale and type. Let $f_j(z_{ij}) = z_{ij}$ or $f_j(z_{ij}) = \log(z_{ij})$ for continuous s_{ij} , with the latter chosen for strictly positive and positively skewed cases. Scale continuous symptoms (after a log transformation if applicable) to have unit variance. Let $f_j(z_{ij}) = 1(z_{ij} > 0)$ for binary s_{ij} , where $1(\cdot)$ is an indicator function taking the value of 1 when the argument is true and 0 when the argument is false. Finally, for (potentially zero-inflated) count s_{ij} let $f_j(z_{ij})$ be a rounding operator such that $f_j(z_{ij}) = 0$ if $z_{ij} < 0$ and $f_j(z_{ij}) = k$ if $k - 1 \leq z_{ij} < k$ [Canale and Dunson, 2013]. Categorical variables may be handled by choosing one category as the baseline and transforming the T categories into $T - 1$ binary variables indicating whether or not the categorical value for that individual took that non-baseline category value (so either none or one of the $T - 1$ variables will take on a value of 1). Other specifications of f would be needed for ordered categorical data to fit within this framework, if desired. Note that of existing models, only Li et al. [2018b] allows for non-binary data, specifically continuous data.

Motivation: It is likely that the full set of symptoms are observations of some lower dimensional syndromic state. Thus, model symptom mean and covariance structure via a smaller set of underlying (unobserved) factors. The number of measured symptoms, P , may be quite large for verbal autopsies (e.g., the 2016 WHO VA instrument [Gen, 2017] asks up to 253 questions for adult and child deaths). Furthermore, many of the causes of interest may have very few observed deaths (e.g., see deaths by cause in the gold standard PHMRC data set in Figure 1). Rather than estimating $P(P + 1)/2$ parameters for each of the C conditional covariance matrices, FARVA introduces a novel hierarchical latent factor model for the latent continuous vector \mathbf{z}_i underlying \mathbf{s}_i . To begin, define:

$$\mathbf{z}_i = \Lambda_{c[i]}(\mathbf{x}_i)\boldsymbol{\eta}_i + \boldsymbol{\epsilon}_i, \quad \boldsymbol{\eta}_i \sim \mathbf{N}(\boldsymbol{\psi}_{c[i]}(\mathbf{x}_i), I_K), \quad \boldsymbol{\epsilon}_i \sim \mathbf{N}(\mathbf{0}_P, \Sigma_0), \quad (4)$$

where $c[i]$ indexes the COD for person i , \mathbf{x}_i are predictors (i.e. covariates) associated with person i , and K is the number of latent factors; in practice K is allowed to be unknown. Here, $\Lambda_{c[i]}(\mathbf{x}_i)$ is a predictor-dependent $P \times K$ factor loadings matrix, $\boldsymbol{\eta}_i$ is a predictor-dependent $K \times 1$ latent factor vector, and $\boldsymbol{\epsilon}_i$ is the $P \times 1$ independent noise vector. The noise covariance Σ_0 is a diagonal matrix having entries $\sigma_j^2, j = 1 \dots P$, with σ_j^2 fixed to equal 1 when s_{ij} is binary or categorical and estimated otherwise. In the above model, $\boldsymbol{\eta}_i$ captures a set of latent syndromes, $\boldsymbol{\psi}_{c[i]}(\mathbf{x}_i)$ the covariate-dependent mean of these latent symptoms for COD $c[i]$, and $\Lambda_{c[i]}(\mathbf{x}_i)$ is a low-rank

description of the symptom correlations for COD $c[i]$ with covariates \mathbf{x}_i . Note that throughout the paper the convention $N(\text{mean}, \text{variance/covariance})$ is used in parameterizing the normally distributed terms.

Since $\boldsymbol{\eta}_i$ is not actually known, dependence is induced in the latent z_i via the marginalization over $\boldsymbol{\eta}_i$. This induced dependence in elements of z_i creates the possibility for dependence to be captured in the likelihood of symptoms given a cause. Specifically, the prior induced on the latent z_i by integrating out $\boldsymbol{\eta}_i$ is:

$$\mathbf{z}_i | y_i \sim N(\Lambda_{c[i]}(\mathbf{x}_i)\boldsymbol{\psi}_{c[i]}(\mathbf{x}_i), \Lambda_{c[i]}(\mathbf{x}_i)\Lambda_{c[i]}(\mathbf{x}_i)' + \Sigma_0), \quad (5)$$

leading to a parsimonious representation of both the mean and the dependence between the P symptoms. An alternative is to define the model as $\mathbf{z}_i = \boldsymbol{\mu}_{c[i]}(\mathbf{x}_i) + \Lambda_{c[i]}(\mathbf{x}_i)\boldsymbol{\eta}_i + \boldsymbol{\epsilon}_i$, with $\boldsymbol{\eta}_i \sim N(\mathbf{0}_K, I_K)$, i.e. with a P -dimensional mean regression. This direct parameterization of the mean has the advantage of allowing a more direct/interpretable way to encode prior information about conditional symptom prevalence, but in the case of large P it becomes unwieldy and computationally intensive.

Motivation: The association between symptoms likely depends on things such as season and decedent age, but modeling a number of covariate-dependent parameters whose size depends on the number of symptoms is computationally intensive. Define a computationally efficient structure by which to model covariate-dependent covariance structure. In order to estimate covariate-dependent factor loadings for large P , decompose $\Lambda_{c[i]}(\mathbf{x}_i)$ to be a weighted combination of a smaller set of basis elements, as in Fox and Dunson [2015]. Namely, let

$$\Lambda_{c[i]}(\mathbf{x}_i) = \Theta_{c[i]}\boldsymbol{\xi}_{c[i]}(\mathbf{x}_i), \quad \Theta_{c[i]} \in \mathbb{R}^{P \times L}, \quad \boldsymbol{\xi}_{c[i]}(\mathbf{x}_i) = \{\xi_{c[i],lk}(\mathbf{x}_i), l = 1, \dots, L, k = 1, \dots, K\}, \quad (6)$$

where $\Theta_{c[i]}$ is the coefficient matrix with weights mapping the smaller set of predictor-dependent basis functions $\boldsymbol{\xi}_{c[i]}(\mathbf{x}_i)$ to the higher-dimensional loadings matrix $\Lambda_{c[i]}(\mathbf{x}_i)$. The number of covariate-dependent parameters to be estimated is $P(P+1)/2$ in direct modeling of the conditional covariance matrix, KP in (4), and KL in (6). Here, K is the dimension of the subspace that is assumed to capture the statistical variability in \mathbf{z} and L is the maximum size of the basis

for any given value of K . Typically $K \ll P$ and $L \ll P$, yielding significant computational savings by using the formulation in (6). If the dependence structure underlying the relationship between symptoms were actually highly complex it would be expected that K and L would need to approach P in size, negating computational advantages of the factor model framework.

Motivation: The size of the underlying basis defining relationships between symptoms isn't actually known. Furthermore, these relationships may be difficult to estimate when the number of observed deaths of a given cause is small. Thus, learn (rather than fix) the basis size while sharing information across causes hierarchically. To share information across causes define the entries of each coefficient matrix $\Theta_c, c = 1, \dots, C$, to share a common population level mean, Δ , across causes. This hierarchical structure serves the purpose of linking factor loadings and increasing robustness when estimating the factor loadings for uncommon causes. Thus similar causes should have similar factor loadings, and loading estimates for rare causes will tend toward the overall population-level mean loadings. Sparsity is induced on the population mean parameter for each entry in the coefficient matrix via the adaptive shrinkage prior of Bhattacharya and Dunson [2011]. The hierarchical shrinkage prior on each element of $\Theta_{c[i]}$ is shown below:

$$\begin{aligned} \theta_{c[i],jl} &\sim \text{N}(\Delta_{jl}, \phi_{\Theta,jl}^{-1} \tau_{\Theta,l}^{-1}), & \phi_{\Theta,jl} &\sim \text{Ga}(\gamma_{\Theta}/2, \gamma_{\Theta}/2), & \tau_{\Theta,l} &= \prod_{h=1}^l \delta_{\Theta,h}, \\ \Delta_{jl} &\sim \text{N}(0, \phi_{\Delta,jl}^{-1} \tau_{\Delta,l}^{-1}), & \phi_{\Delta,jl} &\sim \text{Ga}(\gamma_{\Delta}/2, \gamma_{\Delta}/2), & \tau_{\Delta,l} &= \prod_{h=1}^l \delta_{\Delta,h}, \end{aligned} \quad (7)$$

$$j = 1, \dots, P, l = 1, \dots, L,$$

where L is a conservative upper bound on the basis dimension. The shrinkage prior of Bhattacharya and Dunson [2011] with specification suggested by Durante [2017] is used on the entries of both the within-cause coefficient matrix Θ and across-causes mean matrix Δ . Denoting either Θ or Δ by \cdot , this prior specifies $\phi_{\cdot,jl}$ to be a local precision specific to element j, l and $\tau_{\cdot,l}$ to be a column-specific multiplier. Specifically, this shrinkage prior pulls entries in later columns more strongly toward the mean by letting $\delta_{\cdot,1} \sim \text{Ga}(d_{\cdot,1}, 1)$ and $\delta_{\cdot,h} \sim \text{Ga}(d_{\cdot,2}, 1), h \geq 2$, with $d_{\cdot,2} > 1$. The aim of this prior is to increase the degree of shrinkage as the column index of the matrix grows. In the case of Θ , cause-specific entries are shrunk towards the population mean Δ . In the case of Δ , the population mean is shrunk towards zero. The overall effect is shrinkage of

columns of Θ to 0. The result of this shrinkage is an effective truncation of the number of latent factors because the corresponding rows of the basis $\boldsymbol{\xi}$ will then have insignificant effect in the definition of the resulting mean and covariance of \mathbf{z} . A hallmark of L not being large enough would be columns of Δ close to the L th column remaining large in spite of the shrinkage prior on its entries.

Motivation: The association between symptoms likely depends on covariates, but this covariate dependent relationship may be difficult to learn for causes with a small number of observed deaths. Therefore, model covariate-dependent covariance structure while sharing information across causes hierarchically. The choice of how to model each $\boldsymbol{\xi}_{c[i]}(\mathbf{x}_i)$, the cause-specific $L \times K$ matrix of basis functions of equation (6), to include covariates is flexible. A non-hierarchical nonparametric model can be introduced by choosing independent Gaussian process priors on entries of $\boldsymbol{\xi}$, i.e. $\xi_{c[i],lk} \sim \text{GP}(0, \sigma_\xi(\cdot))$ with $\sigma_\xi(\mathbf{x}, \mathbf{x}')$ an appropriate kernel function. If the covariate included is spatial location, for example $\mathbf{x} = (\text{lat}, \text{lon})'$, a squared exponential covariance kernel with unit variance could be used (the restriction that the kernel has unit variance arises due to identifiability issues with the multiplication with Θ). A separable covariance structure across space and time could also be chosen. The advantage of such a formulation is the ability to model symptom dependence that varies smoothly across space and time, and to infer dependence while predicting COD at locations for which no VAs were recorded. Parametric models for each entry could also be considered by letting $\xi_{c[i],lk}(\mathbf{x}_i) = \boldsymbol{\beta}_{c[i],lk}^T \mathbf{x}_i$. Here $\boldsymbol{\beta}$ is a $B \times 1$ vector, where B is the number of covariates included in the model. This form would be suitable for, e.g., including an indicator variable for whether the i th person died in the hospital, whether the death occurred during the malaria season, or some other relevant information. Aspects of the interviewer, e.g., level of experience, could also be included as predictors. Smoothing splines, piecewise splines, or combinations of parametric and nonparametric forms for predictors can be included, but the level of complexity it is possible and useful to include will be limited by the expressiveness and dimension of the data.

In order to borrow information in the case of small sample sizes within a given cause, introduce a hierarchical prior on elements of the predictor-dependent basis functions $\boldsymbol{\xi}$ and parametric regression parameters $\boldsymbol{\beta}$. Rather than modeling $\boldsymbol{\beta}_{c[i],lk}$ independently for each c , model $\boldsymbol{\beta}_{c[i],lk}$ as

coming from a shared population mean parameter $\boldsymbol{\mu}_{\beta_{lk}}$. For convenience of notation, focus on the case when the covariates of interest are the same for the mean and covariance components of the model. Define the following prior on elements $\xi_{c[i],lk}$ of $\boldsymbol{\xi}_{c[i]}$:

$$\begin{aligned}
\xi_{c[i],lk}(\mathbf{x}_i) &= \boldsymbol{\beta}_{c[i],lk}^T \mathbf{x}_i, \\
\boldsymbol{\beta}_{c[i],lk} &\sim N_B(\boldsymbol{\mu}_{\beta_{lk}}, \Sigma_{\beta_{lk}}), \\
\boldsymbol{\mu}_{\beta_{lk}} &\sim N_B(\boldsymbol{\mu}_0, \Lambda_0), \quad \Sigma_{\beta_{lk}} \sim \text{IW}(\nu_0, S_0), \\
l &= 1, \dots, L, k = 1, \dots, K.
\end{aligned} \tag{8}$$

Motivation: Average symptom observations likely depend on covariates, but this covariate dependent relationship may be difficult to learn for causes with a small number of observed deaths. Model covariate-dependent mean structure while sharing information across causes hierarchically. The choice of how to model $\boldsymbol{\eta}_i$, the cause-specific $K \times 1$ vector of latent syndromes of equation (4), to include covariate information is similarly flexible to that of how to model $\boldsymbol{\xi}$. As with the model for $\boldsymbol{\xi}_{c[i]}(\mathbf{x}_i)$, a non-hierarchical nonparametric model can be introduced by choosing independent Gaussian process priors on entries of $\boldsymbol{\psi}_{c[i]}$. A parametric model is defined by fixing $\psi_{c[i],k} = \boldsymbol{\alpha}_{c[i],k}^T \mathbf{x}_i$. This choice induces the following hierarchical formulation for elements $\eta_{i,k}$ of $\boldsymbol{\eta}_i$:

$$\begin{aligned}
\eta_{i,k}(\mathbf{x}_i) &= \psi_{c[i],k} + \epsilon_{\eta_{ki}} \\
&= \boldsymbol{\alpha}_{c[i],k}^T \mathbf{x}_i + \epsilon_{\eta_{ki}}, \quad \epsilon_{\eta_{ki}} \sim N(0, 1) \\
\boldsymbol{\alpha}_{c[i],k} &\sim N_B(\boldsymbol{\mu}_{\alpha_k}, \Sigma_{\alpha_k}), \\
\boldsymbol{\mu}_{\alpha_k} &\sim N_B(A_0, L_0), \quad \Sigma_{\alpha_k} \sim \text{IW}(\nu_0, D_0), \\
k &= 1, \dots, K.
\end{aligned} \tag{9}$$

When there are no covariates, model elements of $\boldsymbol{\eta}_i$ and $\boldsymbol{\xi}_{c[i]}$ using a mean-only model. Finally, it is possible to include covariates in the model for $\boldsymbol{\xi}_{c[i]}(\cdot)$ that are not included in that for $\boldsymbol{\eta}_i(\cdot)$ or vice versa.

2.3 Posterior computation

The posterior for the FARVA model is not available in closed form, so approximate it via samples obtained from a Markov chain Monte Carlo (MCMC) algorithm. Closed form full conditional distributions of the parameters associated with the model allow the use of a straightforward Gibbs sampler for these draws. The Gibbs sampler has 7 steps.

- *Step 1.* Sample latent syndrome vectors $\{\boldsymbol{\eta}_i\}$ and associated hierarchical regression components.
- *Step 2.* Sample matrices of basis functions $\{\xi_{c[i]}\}$ and associated hierarchical regression components.
- *Step 3.* Update entries of noise matrix Σ_0 .
- *Step 4.* Update entries of the cause-specific coefficient matrix Θ_c for $c = 1, \dots, C$, along with associated shrinkage parameters $\{\phi_{\Theta, jl}\}$ and $\{\delta_{\Theta, h}\}$.
- *Step 5.* Update entries of the population coefficient matrix Δ along with associated shrinkage parameters $\{\phi_{\Delta, jl}\}$ and $\{\delta_{\Delta, h}\}$.
- *Step 6.* Sample latent symptoms z_{ij} for j indexing binary symptoms and $i = 1, \dots, N$.
- *Step 7.* Sample CODs and calculate population CSMF for individuals having unknown COD.

For decedents having unknown COD, it is possible to incorporate knowledge about whether CODs are feasible for a given decedent in the final step of the Gibbs sampler. For example, the model should not be allowed to predict that men have a COD of “maternal” or that women have a COD of “prostate cancer”. If some symptoms are unobserved, it is straightforward to simply impute missing data at each iteration of the Gibbs sampler under the missing at random (MAR) assumption. Full details on each step, posterior computations, hyperparameter settings, and the practical considerations on how the steps are modified for real data are provided in the online supplementary materials.

2.3.1 Performance metrics

The performance metrics used to assess model accuracy are top cause accuracy ACC_1 (10), a measure for how well CODs for individuals are predicted, and CSMF accuracy ACC_{CSMF} (11), a measure for how well the population CSMF is predicted. The top cause accuracy and CSMF accuracy take possible values from 0 to 1, with 1 being best.

$$ACC_1 = \frac{\# \text{ of correct COD being the top cause assignment}}{N} \quad (10)$$

$$ACC_{CSMF} = 1 - \frac{\sum_{c=1}^C |\text{CSMF}_c^{true} - \text{CSMF}_c^{pred}|}{2(1 - \min(\text{CSMF}^{true}))} \quad (11)$$

The CSMF accuracy formula was defined in Murray et al. [2011c], with the idea being that the worst case scenario for CSMF prediction is to put all predicted CSMF weight on the least common cause. This scenario corresponds to a total absolute error of $2(1 - \min(\text{CSMF}^{true}))$. Note that these metrics all rely on there being some hold-out data set for which information on COD is known but can be hidden from the model during training. Results for chance-corrected concordance, a metric with a 0 value corresponding to the performance expected of random uniform guessing, are included in the online supplementary materials.

2.4 Simulations

Commonly, work on VA based COD algorithms jump immediately to training/testing using samples from the PHMRC data set. This approach has the advantage of allowing questions such as “How do algorithms trained in one context and tested in another perform?” and “What causes are easier/harder to predict?”; it places the emphasis on performance of algorithms with real data. However, the underlying mean/covariance of symptoms in these resampled PHMRC data sets are unknown. This limitation makes it difficult to manipulate and explore how differing symptom level mean and covariance structures impact model performance. To address this question, the current work includes simulated scaled down data sets having just 928 observations, 21 “symptoms”, and 4 “causes”. Via different generative processes, it is possible to explore various structures of cause-specificity and covariate dependence for the simulated datasets’ mean and covariance.

		Artificial data structure		
Simulation		Mean structure	Covariance structure	Data type
No covariate information included	<i>a</i>	S	C, I	B
	<i>b</i>	S	C, D	B
	<i>c</i>	C	S, D	B
	<i>d</i>	S	S, D	B
Covariate information included	<i>e</i>	S, V	C, I	B
	<i>f</i>	C	S, D, V	B
	<i>g</i> ₁	S, V	S, D, V	B
	<i>g</i> ₂	S, V	S, D, V	M
	<i>g</i> ₃	S, V	S, D, V	T

Table 1: In the table above S denotes cause-specific, C denotes common across causes; I denotes independent, D denoted non-independent; V denotes covariate-dependent; B denotes binary, M denotes mixed, and T denotes continuous. For example, simulation *d* has cause-specific (S) mean structure and cause-specific (S) dependent (D) covariance structure, and the data type is binary (B). The simulation letter denotes that 1000 data sets are sampled for that letter. For example, simulations *g*₁, *g*₂, and *g*₃ are based on the same underlying data set so the same inputs are provided for each to the BF, InSilicoVA, NBC, and Tariff methods, but different inputs are given to FARVA (*g*₁ uses binary inputs, *g*₂ uses mixed inputs, and *g*₃ uses continuous inputs).

Table 1 shows detailed information about the various simulation configurations. For each simulation configuration sample 1000 data sets, a number chosen to balance the considerations of Monte Carlo error and computation time, and run FARVA, Kunihamas Bayesian factor (BF) model, open source Tariff, InSilicoVA, and the naive Bayes classifier (NBC). Broadly speaking, there are two classes of configuration:

1. No covariate information included: Simulations *a* through *d*, with various combinations of cause-specificity in mean/covariance. FARVA is likely to only do as well as existing methods.
2. Covariate information included: Simulations *e* through *g*, with various combinations of cause-specificity in mean/covariance, with covariate effects. FARVA is expected to outperform existing methods.

Note that although simulation *g* includes mixed and continuous versions of the data set for testing with FARVA, all other methods compared can use only binary data. More details of how data are simulated and visuals of the impact of various simulation settings are provided in the online supplementary materials.

Simulations using the PHMRC data are also performed. To begin, the data are read into **R** using the command `read.csv(openVA::getPHMRC_url("adult"))` (yielding 7841 observations) and the one observation for which a decedent has age < 12 is removed (leaving 7840 adult deaths).

The data are then divided by site (Andhra Pradesh, India ; Bohol, Philippines; Dar es Salaam, Tanzania; Mexico City, Mexico; Pemba Island, Tanzania; and Uttar Pradesh, India). For each site the following is repeated 100 times: First, site-specific data are split into 75% training, 25% test. Then, data cleaning steps used in the **OpenVA** software were performed, i.e. all variables converted to dichotomous symptoms matching those used in InterVA algorithm. Specifically, the adult PHMRC data was processed using the `ConvertData.phmrc()` command with `cutoff = "default"` and `cause = "va34"`. Variables were then cleaned such that symptoms having a high missingness rate (specifically, over 95% missing) or zero variability (i.e., all respondents had the same answer) were removed from analysis. Only the subset of causes included in the training data set were included as possible causes in each analysis. Finally, each model is run, with FARVA including whether or not each decedent was an elder (≥ 65) as a covariate. The competitor methods included are the same as those used in the simulated data runs. The InterVA and King Lu methods were not included as competitors, as both were found by Kunihaman et al. [2018] to have consistently poor performance relative to state of the art.

To explore cause-specific and potentially covariate-dependent prevalence and patterns of association between symptoms, the FARVA model is run using the full PHMRC data set (i.e., including data from across all sites and with no held-out test data) with (1) no covariates included and (2) a covariate for whether or not each decedent was an elder included. This exploration is a novel contribution to the VA literature. Li et al. [2018b] described overall patterns of association between symptoms, but their model does not allow for covariance structure to differ across causes. No previous paper has explored the difference in patterns of association between symptoms across CODs (although the BF model would also allow such an analysis, none was performed in Kunihaman et al. [2018]). Furthermore, as no previous models have allowed for covariate inclusion, the question of how the mean or covariance structure differs within (or across) COD(s) for a given covariate has yet to be addressed for any covariate. Note that results here are meant to be illustrative rather than exhaustive, highlighting the utility of the FARVA model for exploring both the symptom level mean structure and patterns of association. Further simulation run details are provided in the online supplementary materials.

3 Results and discussion

Performance of both the simulated and the PHMRC data runs are discussed below. In summary, explicitly accounting for covariate dependence in the model does improve predictive performance in both simulated and real data. The degree to which performance improves depends on the strength of the relationship between a covariate and symptom prevalence and/or associations.

3.1 Simulation performance

Two sets of simulations are considered. In the first, no covariate information is included or modeled (simulations *a* through *d*). In the second, a single binary covariate is introduced as a modifier of the mean and/or covariance structure of symptoms (simulations *e* through *g*₃). See the online supplementary materials for visual examples of the symptom mean and covariance structure from each simulation setting, and for performance as a function of degree of cause-specificity, and for plots of performance as a function of covariate dependence and proportion of data allowed to be continuous.

3.1.1 Simulations with no covariate dependence

Simulation *a* fixes cause-specific symptom mean structure for each cause and shared **independent** covariance structure across causes. This simulation is designed to mimic a scenario in which the conditionally independent assumption is valid, and the only information about cause of death comes from symptom prevalence. The models allowing the specification of a non-independent conditional covariance matrix (FARVA and BF) perform comparably to models assuming conditional independence. Simulation *b* is similar to simulation *a* in that the only information on COD is found in the differing mean structure across causes. The difference is that symptoms are assumed to have a shared **dependent** covariance structure across causes. Both FARVA and BF are able to learn this shared covariance structure, and both perform slightly better than models assuming conditional independence.

Simulation *c* fixes a common symptom mean structure across causes and symptom covariance structure specific to each cause. In other words, all of the information differentiating CODs

Simulation		FARVA	BF	VA model InSilico	NBC	Tariff
ACC ₁	<i>a</i>	0.524 (0.047)	0.518 (0.047)	0.493 (0.069)	0.528 (0.046)	0.50 (0.045)
	<i>b</i>	0.532 (0.045)	0.527 (0.045)	0.470 (0.068)	0.522 (0.048)	0.498 (0.045)
	<i>c</i>	0.635 (0.039)	0.634 (0.040)	0.268 (0.065)	0.275 (0.035)	0.262 (0.040)
	<i>d</i>	0.711 (0.036)	0.712 (0.037)	0.420 (0.070)	0.468 (0.042)	0.444 (0.043)
ACC _{CSMF}	<i>a</i>	0.894 (0.013)	0.895 (0.014)	0.841 (0.104)	0.908 (0.024)	0.903 (0.027)
	<i>b</i>	0.895 (0.014)	0.898 (0.016)	0.831 (0.104)	0.901 (0.034)	0.902 (0.030)
	<i>c</i>	0.913 (0.014)	0.915 (0.015)	0.650 (0.148)	0.858 (0.040)	0.808 (0.087)
	<i>d</i>	0.926 (0.015)	0.929 (0.016)	0.784 (0.139)	0.896 (0.030)	0.892 (0.031)

Table 2: Above are the mean (SD) of the top cause accuracy (ACC₁) and CSMF accuracy (ACC_{CSMF}) for the 1000 data sets sampled for each simulation having no covariate dependence. The highest performing model is indicated by a bolded mean. Note that FARVA and BF perform quite similarly with regards to both ACC₁ and ACC_{CSMF}, as expected. See Table 1 for data structure for each simulation setting.

is found in the covariance structure. In this setting, models making the conditional independence assumption have no information by which to make a COD determination, and as expected FARVA and BF are the only models to perform better than simple uniform guessing. Simulation *d* fixes a symptom mean and covariance structure specific to each cause. In other words, information about the COD may be found in both the mean and the covariance structure of symptoms. As expected, FARVA and BF outperformed the models that only utilize information about symptom means. Also, FARVA and BF outperformed their own metrics in previous simulation runs, illustrating that both the mean and the covariance have the potential to contain valuable information.

3.1.2 Simulations with covariate dependence

Simulation *e* fixes cause-specific symptom mean structure that varies with covariates for each cause and shared independent covariance structure across causes. This simulation is designed to mimic a scenario in which the conditionally independent assumption is valid, and COD-specific symptom prevalence is modified by a single binary covariate. FARVA can utilize this covariate information to more accurately capture cause-specific symptom mean structure for all individuals, and as expected it has the highest performance. Simulation *f* fixes a common symptom mean structure across causes and symptom covariance structure that varies with covariates specific to each cause. Again, only FARVA and BF are expected to do better than chance, and of the two only FARVA can utilize this covariate information to more accurately capture cause-specific symptom association structure for all individuals. Simulation *g* sets both the mean and

Simulation		FARVA	BF	VA model InSilico	NBC	Tariff
ACC ₁	<i>e</i>	0.442 (0.039)	0.397 (0.036)	0.332 (0.079)	0.389 (0.037)	0.372 (0.037)
	<i>f</i>	0.578 (0.038)	0.496 (0.038)	0.255 (0.071)	0.264 (0.032)	0.258 (0.038)
	<i>g</i> ₁	0.653 (0.035)	0.552 (0.038)	0.333 (0.075)	0.392 (0.036)	0.375 (0.038)
	<i>g</i> ₂	0.674 (0.035)	—	—	—	—
	<i>g</i> ₃	0.749 (0.033)	—	—	—	—
ACC _{CSMF}	<i>e</i>	0.883 (0.010)	0.881 (0.011)	0.647 (0.184)	0.884 (0.030)	0.883 (0.031)
	<i>f</i>	0.902 (0.013)	0.894 (0.014)	0.647 (0.161)	0.862 (0.037)	0.809 (0.086)
	<i>g</i> ₁	0.913 (0.013)	0.902 (0.014)	0.649 (0.180)	0.882 (0.030)	0.882 (0.031)
	<i>g</i> ₂	0.915 (0.013)	—	—	—	—
	<i>g</i> ₃	0.924 (0.013)	—	—	—	—

Table 3: Above are the mean (SD) of the top cause accuracy (ACC₁) and CSMF accuracy (ACC_{CSMF}) for the 1000 data sets sampled for each simulation having covariate dependence in the mean, covariance, or both. Recall that different inputs are given to FARVA for the *g* simulations (*g*₁ uses binary inputs, *g*₂ uses mixed inputs, and *g*₃ uses continuous inputs); the results for the non-FARVA models are shared across each *g*. See Table 1 for other information about the data structure for each simulation setting. The highest performing model is indicated by a bolded mean. The proportion of datasets for which FARVA outperformed BF for simulations *e* through *g*₃ is 0.91, 1.00, 1.00, 1.00, and 1.00 for ACC₁ and 0.61, 0.82, 0.87, 0.88, and 0.94 for ACC_{CSMF}, respectively.

covariance of symptoms to depend on cause and vary with a binary covariate. This simulation illustrates that FARVA does best when both the mean and the covariance depend on a covariate, and its performance improves when truly continuous data are included in the model as such.

3.2 PHMRC predictive performance

Top cause accuracy results for the 100 test/train splits of each site-specific PHMRC data set are shown in Figure 4. FARVA outperforms its competitors with regards to top cause accuracy at each site. Notably, FARVA shows improvement relative the BF model in each setting.

CSMF accuracy results are shown in Figure 5. FARVA outperforms its competitors with regards to CSMF accuracy in each site. As before, FARVA shows an improvement in performance over the BF model in each setting. Unsurprisingly, the regions of highest individual performance gain for FARVA are also those with highest CSMF performance gain (e.g., Mexico City and Uttar Pradesh). However, in some contexts the BF model is able to allocate probability across true causes in test data nearly as well as FARVA (e.g., Pemba Island and to a lesser extent Bohol). See the online supplementary materials for histograms showing the difference in top cause and CSMF accuracy between FARVA and BF in each train/test split

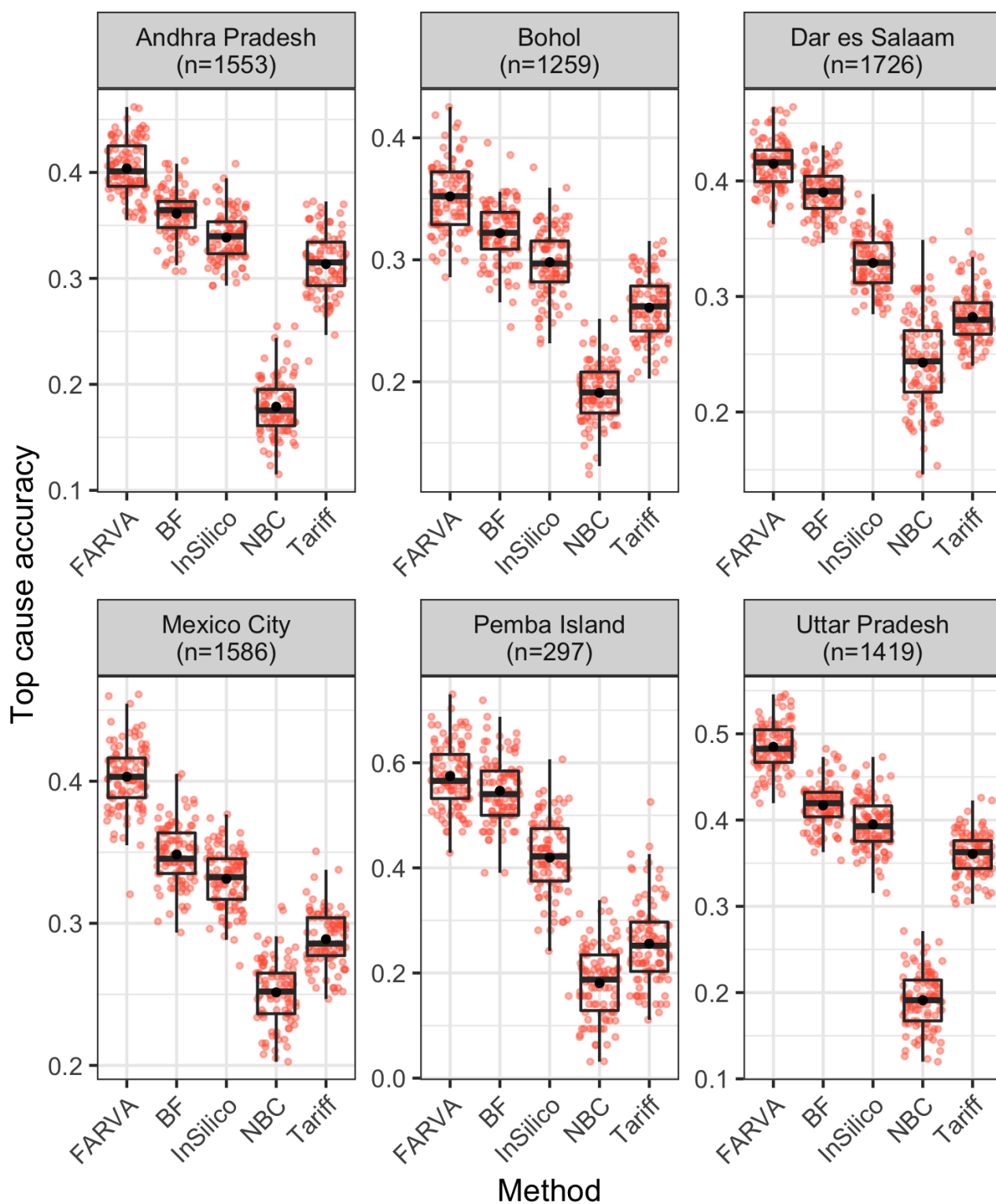


Figure 4: Top cause accuracy for PHMRC data over 100 test/train splits at each site. The centered solid point (horizontal bar) shows the mean (median) across test/train splits, for which individual performance results are shown as semi translucent horizontally jittered points. Each method shares data processing steps, but decedent age (≥ 65) is included in FARVA as a binary covariate. For each site (read left to right, top to bottom), the FARVA model outperforms the BF model for 88, 75, 81, 97, 61, and 99% of the test/train splits.

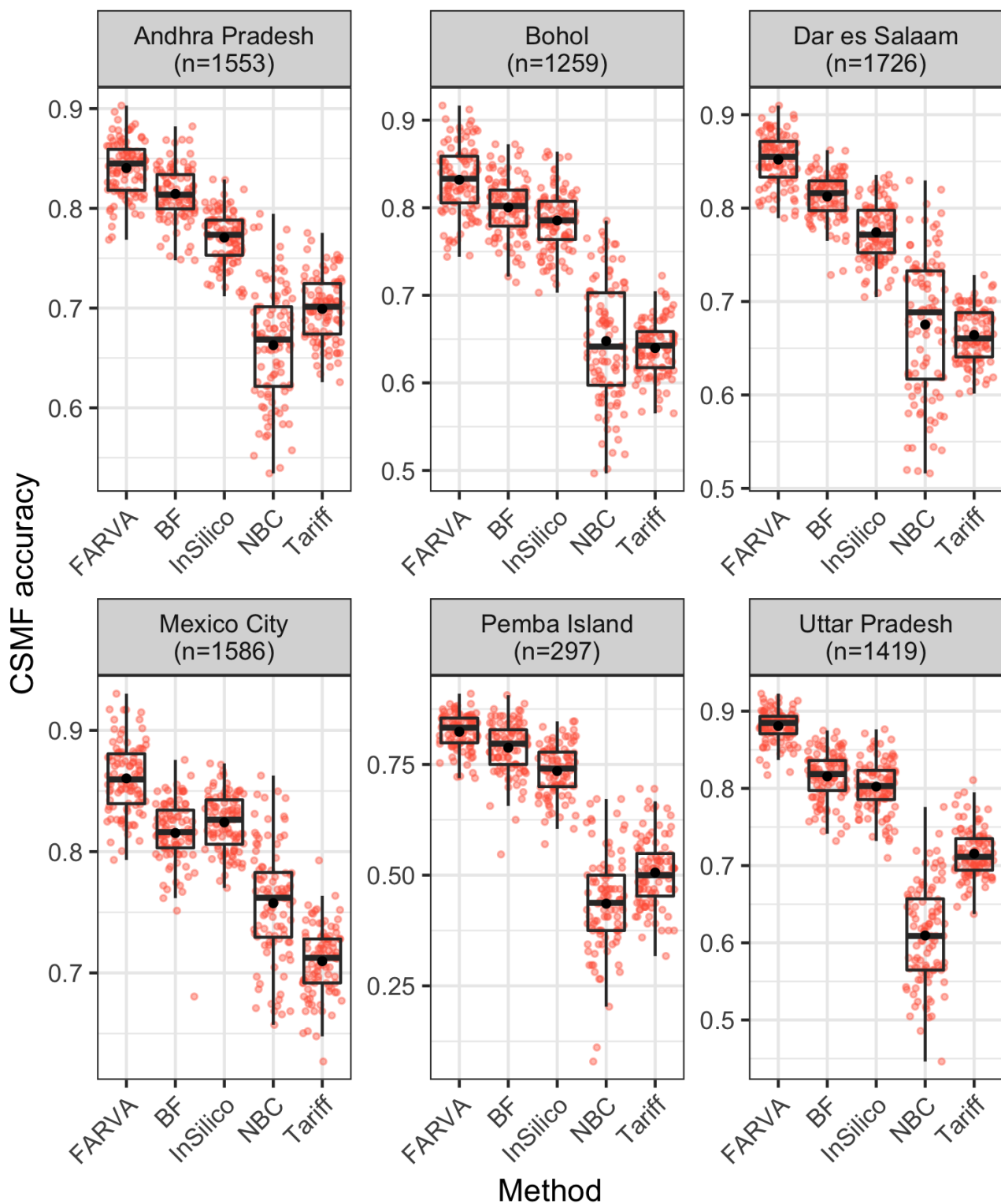


Figure 5: CSMF accuracy for PHMRC data over 100 test/train splits at each site. The centered solid point (horizontal bar) shows the mean (median) across test/train splits, for which individual performance results are shown as semi translucent horizontally jittered points. Each method shares data processing steps, but decedent age (≥ 65) is included in FARVA as a binary covariate. For each site (read left to right, top to bottom), the FARVA model outperforms the BF model for 72, 68, 87, 86, 64, and 97% of the test/train splits.

3.3 Inference on VA questionnaire data

Of interest in addition to prediction is model-based inference on the structure of responses within VA questionnaires. The FARVA model allows for both the mean and the covariance structure of the latent symptom vector \mathbf{z}_i to be interrogated. In the following examples the same set of binary symptoms as those used to train the model in the PHMRC predictive ability assessment are considered. The PHMRC variable names and questions are included in full in the online supplementary materials.

3.3.1 Symptom-level mean

First consider an intercept-only FARVA model, i.e. one in which x_i is set to 1 in equations (8) and (9), run using all 7840 adult deaths in the PHMRC data set. Figure 6 illustrates model inference on $\mathbb{E}[\mathbf{z}_{c[i]}]$, the mean of the latent symptom vector $\mathbf{z}_{c[i]}$, for some select symptoms and causes. The most important thing to notice about the example is that the latent symptom posterior means differ by cause. For example, samples of $\mathbb{E}[z_{c[i], \text{Weight loss}}]$ tend to be positive for CODs cirrhosis, pneumonia, and prostate cancer, and negative for COD homicide, implying that weight loss occurs less frequently for homicide deaths. These learned cause-specific patterns of latent symptom means, which differ across CODs, are a part of what drives the model’s prediction ability. The online supplementary materials provide additional visuals showing the estimated posterior mean and 95% credible interval for the $\mathbf{z}_{c[i]}$ vector in the intercept-only FARVA model for two example CODs.

Next consider a FARVA model run using all training data with the binary covariate of decedent age (≥ 65) included, i.e. one in which \mathbf{x}_i is set to $(\mathbf{1}_{\text{age}[i] \geq 65}, \mathbf{1}_{\text{age}[i] < 65})'$ in equations (8) and (9). Figure 7 provides an example of FARVA’s potential to elucidate differences in individual response patterns within COD by covariate, showing $\mathbb{E}[z_{c[i], j}]$ for select symptoms and CODs. The included non-injury-related latent symptom means for homicide deaths are pulled closer to zero for older decedents, likely due to the small number of observed elder deaths due to homicide combined with the general trend across CODs for senior decedents to experience more constellations of symptoms. While symptom patterns also differ by age for pneumonia deaths, they are similar for the other CODs considered in this example, implying that not all conditional

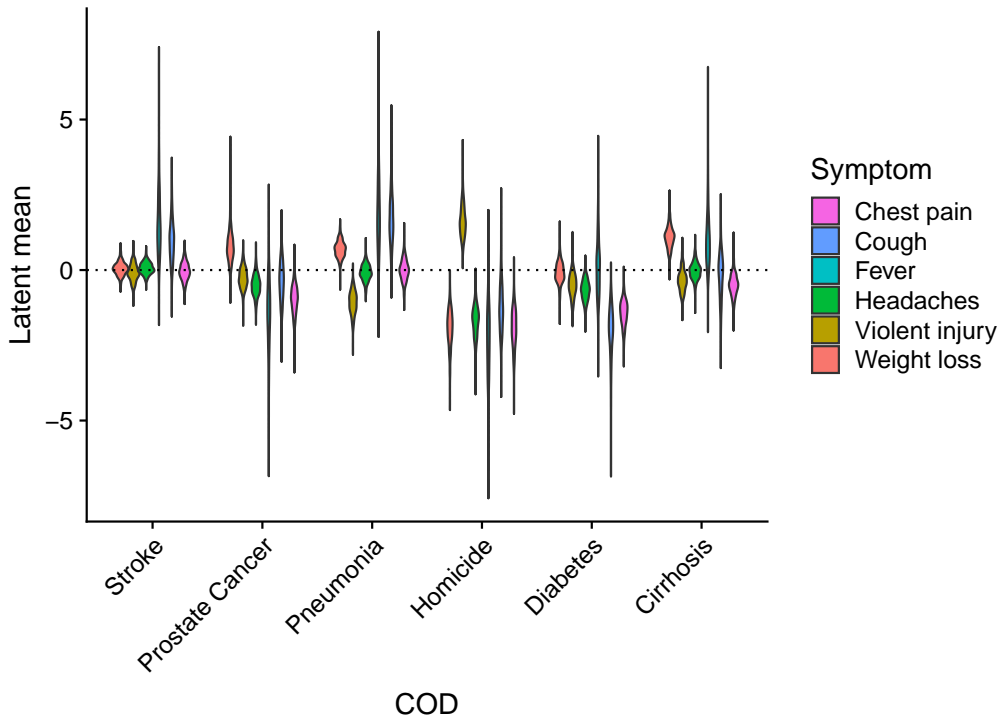


Figure 6: Violin plot visualizing samples of $\mathbb{E}[z_{c[i],j}]$ for CODs cirrhosis ($n = 313$), diabetes ($n = 414$), homicide ($n = 167$), pneumonia ($n = 540$), prostate cancer ($n = 48$), and stroke ($n = 630$) for select symptoms. An expected latent symptom mean being positive (negative) corresponds to more (less) expected observed “Yes” responses for those symptoms.

symptom means are differentially expressed by the different age groups.

When age is included as a covariate, it acts as a moderator of the latent mean pattern for a given cause and symptom. The most notable feature of the pattern of symptoms for elders is that they appear more similar across CODs. This is consistent with the hypothesis that elders tend to have more diffuse symptoms from a myriad of ailments, not just a pointed set of symptoms leading to a specific diagnosis. The latent mean $\mathbb{E}[z_{c[i],j}]$ is significantly greater than (less than) 0 for 3% (63%) of the 4658 possible symptom-cause combinations (137 included symptoms \times 34 causes) for non-elders, but only 1% (59%) of the possible symptom-cause combinations for elders. This phenomenon, although slight, illustrates that FARVA is able to be more focused for younger individuals and spread probability more diffusely for elders, who tend to exhibit a wider array of symptoms across causes. Such behavior could contribute to the improvement in top cause accuracy and CSMF accuracy seen in the previous section.

3.3.2 Symptom-level association

Li et al. [2018a] consider inference on overall symptom-level covariance in verbal autopsy data

for continuous symptoms, but the results are not cause-specific. Kuniyama et al. [2018] discuss

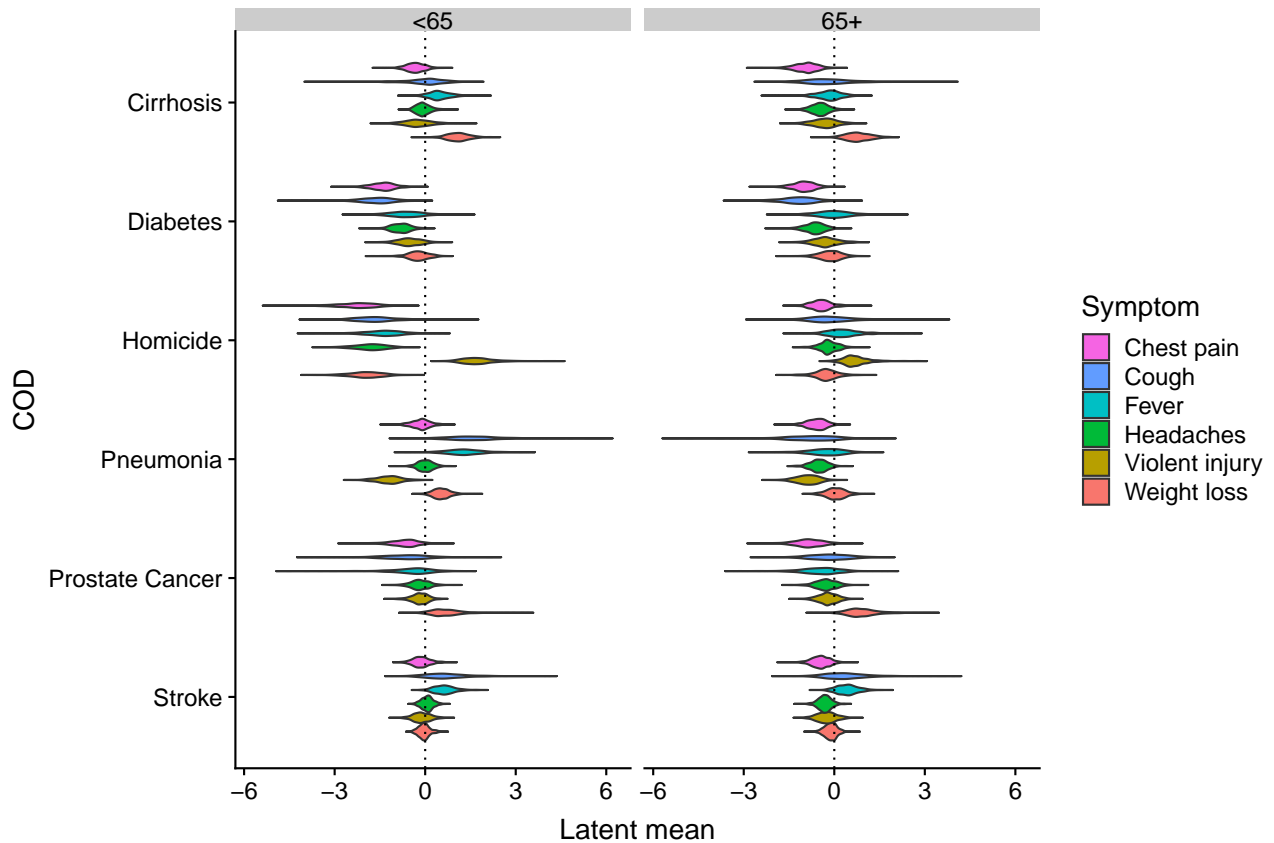


Figure 7: Violin plot visualizing samples of $\mathbb{E}[z_{c[i],j}]$ for CODs cirrhosis ($n_{\geq 65} = 49$, $n_{<65} = 260$), diabetes ($n_{\geq 65} = 116$, $n_{<65} = 293$), homicide ($n_{\geq 65} = 5$, $n_{<65} = 161$), pneumonia ($n_{\geq 65} = 193$, $n_{<65} = 341$), prostate cancer ($n_{\geq 65} = 29$, $n_{<65} = 19$), and stroke ($n_{\geq 65} = 288$, $n_{<65} = 332$) for select symptoms.

a model-based version of Cramer’s V, but this metric is only applicable to binary symptoms. To the authors’ knowledge, no work has the ability to perform model-based inference on cause-specific covariance in VA data of mixed type.

Again, first consider an intercept-only FARVA model run using all training data. Figure 8 provides an example of model inference on $\text{Cov}(z_{c[i],j}, z_{c[i],k})$ for pairs of symptoms j and k , which can be thought of as the latent symptom covariance. These learned patterns of latent symptom covariances capture additional information beyond just symptom prevalence that the model can use to differentiate between CODs.

When age is included as a covariate, it acts as a weak moderator of the latent covariance pattern for given pair of symptoms within a cause (figures included in online supplementary materials). Of note is that the patterns of association within a COD are similar across age groups, but the strength of association tends to be weaker for younger decedents. Furthermore, the credible intervals tend to be wider for older decedents. This finding differs from the exploratory finding

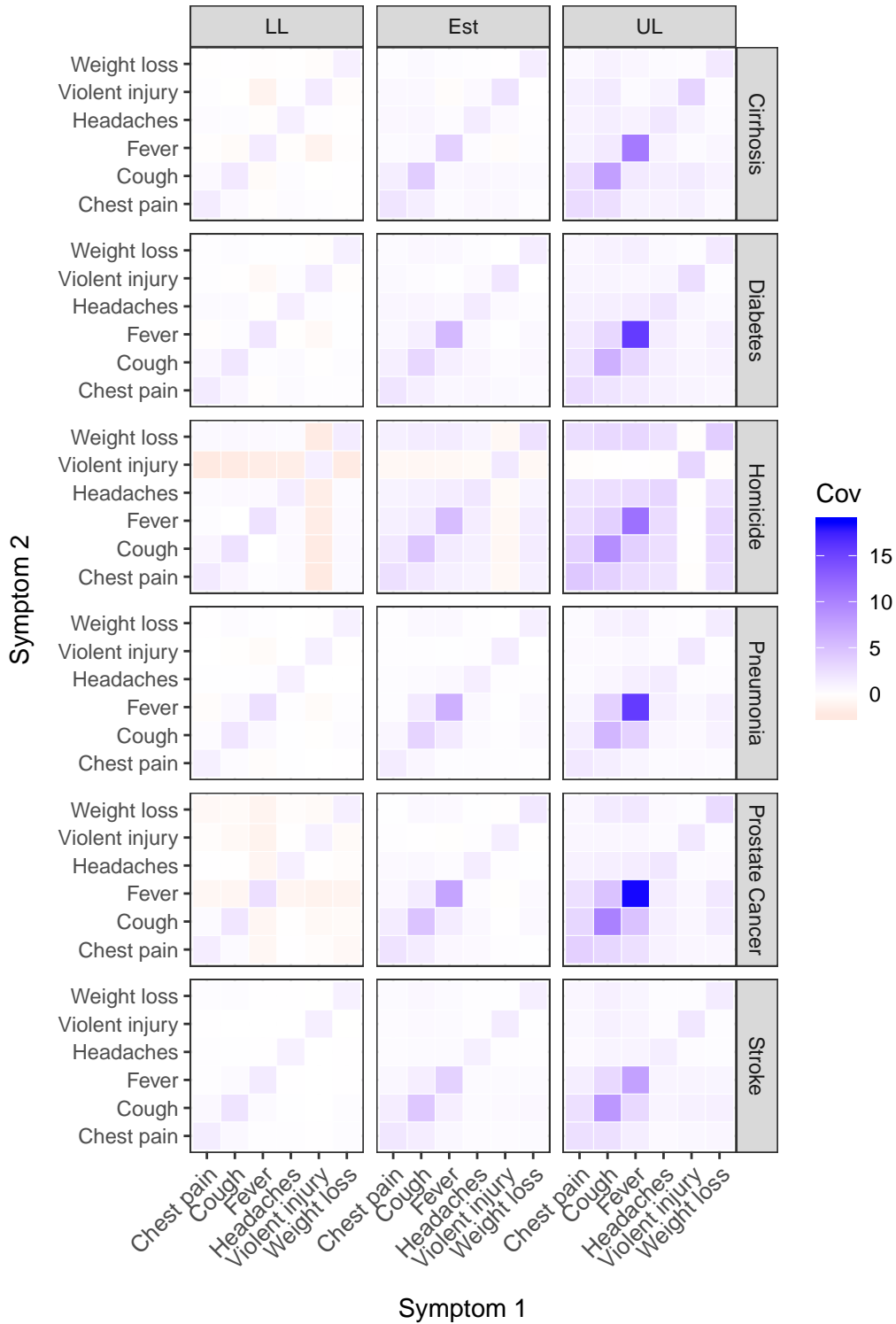


Figure 8: Correlation plot visualizing the mean and lower/upper 95% credible interval of $\text{Cov}(z_{c[i],j}, z_{c[i],k})$ for CODs cirrhosis ($n = 313$), diabetes ($n = 414$), homicide ($n = 167$), pneumonia ($n = 540$), prostate cancer ($n = 48$), and stroke ($n = 630$) for select symptoms. An expected latent covariance mean being positive (negative) corresponds to observed “Yes” or “No” responses for those symptoms to (not) co-occur. For example, samples of $\text{Cov}(z_{c[i],\text{Cough}}, z_{c[i],\text{Chest pain}})$ tend to be positive across all CODs, implying that the symptoms cough and chest pain tend to co-occur. On the other hand, violent injury tends not to be associated with the other symptoms shown, and is significantly negatively associated with these symptoms in the case of homicide deaths.

that, across all causes of death, age tends to weaken symptom associations. The difference is due to the conditional nature of these covariance matrices; rather than marginalizing over COD, these symptom associations are conditional on a COD. It is likely that the combination of slightly stronger average covariance along with a wider credible interval is due to the tendency for elderly individuals to be “hit harder” by an illness, i.e. to suffer from a large number of the common symptoms for that illness. At the same time, they likely also tend to have many other symptoms unrelated to their COD, and make up a smaller proportion of deaths for each COD, hence the increased uncertainty.

4 Discussion

The PHMRC data set, while useful for model testing and validation, has some drawbacks. Deaths clear enough to be considered “gold standard” by the PHMRC may not be representative of the population of community deaths, relationships between symptoms/causes learned in one context may not transfer to new contexts (location/time), and, relevant to this work, few potential covariates are recorded. More generally, information in VA data is only as reliable as the interviewee’s knowledge. Finally, the question of how to merge different questionnaires (e.g., the adult/child PHMRC form) and select/prioritize symptoms for inquiry remains an open area of research.

For comparability to recent competing methods, the real data analysis of this paper considered only the binary symptoms initially chosen by Byass et al. [2012]. However, the selection of which symptoms to include and whether to include them as binary or continuous variables is an area of open and important research. This issue is not unique to FARVA, and a rigorous consideration of the importance of various symptoms in assigning COD across models would be useful for both model performance and to lower the burden placed on interviewees (a reduced interview set that takes less time would be preferred). An area of potential improvement to the FARVA model itself would be incorporating a prior that could encourage row-level sparsity in the cause-specific loadings matrix $\Lambda_{c[i]}$. This addition could help the model better capture the likely realistic idea that many symptoms may be unimportant to assigning a cause, and could also help assess the relevance of symptoms for inclusion on future questionnaires.

Training on data from one (or multiple) setting(s) and testing in another is common practice for VA algorithms (e.g., using data from Dar es Salaam to train a model, then using test data from Pemba Island). Recent work by Clark et al. [2018] has quantified the effect on predictive performance of this practice. They show that the impact of the information about the joint distribution between symptoms and causes is at least as high as that of the underlying algorithm’s logic. In other words, existing algorithms cannot correct for discrepancy between the joint distribution between symptoms and causes in a new site relative to the body of training data. Work by Datta et al. [2018] has focused on accounting for local discrepancy when learning the CSMF at a site with limited training data. It is likely that some (although almost certainly not all) of the variation between sites is systematic and related to measurable features such as seasonal difference, endemicity of various pathogens, urbanicity, etc. If so, some of this decline in predictive performance could be corrected for explicitly in a model like FARVA via the inclusion of region-specific or individual-level covariates in a model. Exploring which covariates help model transferability is a potential future area of research.

The work of McCormick, Clark, Li, and the rest of their team has been pivotal in universalizing algorithm-assigned COD using VA data. In large part, this is due to his team’s excellent documentation and code base. The FARVA team strives to maintain similarly high standards of documentation and usability of the code under hopes that it will be friendly to the broader VA community. Algorithm code and a user manual for the FARVA model are available at <https://github.com/kelrenmor/farva>.

5 Acknowledgments

The authors are grateful to John A. Crump, Manuela Carugati, Matthew P. Rubach, and Michael J. Maze for introducing us to the problem and inspiring us to think about methodological developments, and for helpful discussions with them and the rest of the Investigating Febrile Deaths in Tanzania (INDITe) team. This research was partly supported by the US National Institutes of Health (R01AI121378) for the INDITe project and by the Department of Energy Computational Science Graduate Fellowship (DE-FG02-97ER25308). The funders had no role in study design, data collection and analysis, decision to publish, or preparation of the manuscript.

A Appendix

Let U^* denote the group of individuals having unknown COD. For person $i^* \in U^*$, calculate

$$\pi(y_{i^*} = c | \mathbf{s}_{i^*}) = \frac{\pi(\mathbf{s}_{i^*} | y_{i^*} = c) \pi(y_{i^*} = c)}{\sum_{c'=1}^C \pi(\mathbf{s}_{i^*} | y_{i^*} = c') \pi(y_{i^*} = c')} \quad (\text{A.1})$$

for each $c = 1, \dots, C$, and sample from the resulting discrete distribution. The online supplemental materials discuss how this value is calculated in practice, along with the computational expense of Monte Carlo integration over $\boldsymbol{\eta}_i$ vs. direct sampling.

Then compute the population distribution of causes for individuals in U^* as:

$$\text{CSMF}_{U^*} = \left(\frac{1}{|U^*|} \sum_{i^* \in U^*} 1(y_{i^*} = 1), \dots, \frac{1}{|U^*|} \sum_{i^* \in U^*} 1(y_{i^*} = C) \right). \quad (\text{A.2})$$

The above comprises a sample of the CSMF for the set U^* . Note (A.2) is different than the posterior distribution of cause-specific probabilities, which includes individuals having both known and unknown CODs and is given by:

$$\begin{aligned} & \{\Pr(y_i = 1), \dots, \Pr(y_i = C)\} \mid \{\Lambda_{c[i]}\}, \{\boldsymbol{\eta}_i\}, \Sigma_0 \\ & \sim \text{Dirichlet} \left(a_1 + \frac{1}{N} \sum_{i=1}^N 1(y_i = 1), \dots, a_C + \frac{1}{N} \sum_{i=1}^N 1(y_i = C) \right). \end{aligned} \quad (\text{A.3})$$

References

- A Bhattacharya and D B Dunson. Sparse Bayesian infinite factor models. *Biometrika*, 98(2): 291–306, 2011.
- Peter Byass, Daniel Chandramohan, Samuel J Clark, Lucia D’ambruoso, Edward Fottrell, Wendy J Graham, Abraham J Herbst, Abraham Hodgson, Sennen Hounton, Kathleen Kahn, et al. Strengthening standardised interpretation of verbal autopsy data: the new InterVA-4 tool. *Global Health Action*, 5(1):19281, 2012.
- Antonio Canale and David B Dunson. Nonparametric Bayes modelling of count processes. *Biometrika*, 100(4):801–816, 2013.

- Samuel J Clark, Zehang Li, and Tyler H McCormick. Quantifying the contributions of training data and algorithm logic to the performance of automated cause-assignment algorithms for verbal autopsy. *arXiv preprint arXiv:1803.07141*, 2018.
- John A Crump, Anne B Morrissey, William L Nicholson, Robert F Massung, Robyn A Stoddard, Renee L Galloway, Eng Eong Ooi, Venance P Maro, Wilbrod Saganda, Grace D Kinabo, et al. Etiology of severe non-malaria febrile illness in northern tanzania: A prospective cohort study. *PLoS neglected tropical diseases*, 7(7):e2324, 2013.
- Abhirup Datta, Jacob Fiksel, Agbessi Amouzou, and Scott Zeger. Local calibration of verbal autopsy algorithms. *arXiv preprint arXiv:1810.10572*, 2018.
- Daniele Durante. A note on the multiplicative gamma process. *Statistics & Probability Letters*, 122:198–204, 2017.
- Emily B Fox and David B Dunson. Bayesian nonparametric covariance regression. *The Journal of Machine Learning Research*, 16(1):2501–2542, 2015.
- Manual for the training of interviewers on the use of the 2016 WHO VA instrument*. Geneva: World Health Organization, 2017. License: CC BY-NC-SA 3.0 IGO.
- Global Burden of Disease Collaborative Network. Global burden of disease study 2016 (GBD 2016) results. <http://ghdx.healthdata.org/gbd-results-tool>, 2017.
- Spencer L James, Abraham D Flaxman, and Christopher JL Murray. Performance of the Tariff Method: validation of a simple additive algorithm for analysis of verbal autopsies. *Population Health Metrics*, 9(1):31, 2011.
- Gary King, Ying Lu, et al. Verbal autopsy methods with multiple causes of death. *Statistical Science*, 23(1):78–91, 2008.
- Tsuyoshi Kuniyama, Zehang Richard Li, Samuel J Clark, and Tyler H McCormick. Bayesian factor models for probabilistic cause of death assessment with verbal autopsies. *arXiv preprint arXiv:1803.01327*, 2018.
- Zehang Richard Li, Tyler H McCormick, and Samuel J Clark. Bayesian joint spike-and-slab graphical lasso. *arXiv preprint arXiv:1805.07051*, 2018a.

- Zehang Richard Li, Tyler H McCormick, and Samuel J Clark. Using Bayesian latent Gaussian graphical models to infer symptom associations in verbal autopsies. *arXiv preprint arXiv:1711.00877*, 2018b.
- Tyler H McCormick, Zehang Richard Li, Clara Calvert, Amelia C Crampin, Kathleen Kahn, and Samuel J Clark. Probabilistic cause-of-death assignment using verbal autopsies. *Journal of the American Statistical Association*, 111(515):1036–1049, 2016.
- Pierre Miasnikof, Vasily Giannakeas, Mireille Gomes, Lukasz Aleksandrowicz, Alexander Y Shestopaloff, Dewan Alam, Stephen Tollman, Akram Samarikhalaj, and Prabhat Jha. Naive Bayes classifiers for verbal autopsies: comparison to physician-based classification for 21,000 child and adult deaths. *BMC Medicine*, 13(1):286, 2015.
- Christopher JL Murray, Spencer L James, Jeanette K Birnbaum, Michael K Freeman, Rafael Lozano, and Alan D Lopez. Simplified Symptom Pattern Method for verbal autopsy analysis: multisite validation study using clinical diagnostic gold standards. *Population Health Metrics*, 9(1):30, 2011a.
- Christopher JL Murray, Alan D Lopez, Robert Black, Ramesh Ahuja, Said Mohd Ali, Abdullah Baqui, Lalit Dandona, Emily Dantzer, Vinita Das, Usha Dhingra, et al. Population health metrics research consortium gold standard verbal autopsy validation study: design, implementation, and development of analysis datasets. *Population Health Metrics*, 9(1):27, 2011b.
- Christopher JL Murray, Rafael Lozano, Abraham D Flaxman, Alireza Vahdatpour, and Alan D Lopez. Robust metrics for assessing the performance of different verbal autopsy cause assignment methods in validation studies. *Population Health Metrics*, 9(1):28, 2011c.
- Christopher JL Murray, Rafael Lozano, Abraham D Flaxman, Peter Serina, David Phillips, Andrea Stewart, Spencer L James, Alireza Vahdatpour, Charles Atkinson, Michael K Freeman, et al. Using verbal autopsy to measure causes of death: the comparative performance of existing methods. *BMC Medicine*, 12(1):5, 2014.
- Erin K Nichols, Peter Byass, Daniel Chandramohan, Samuel J Clark, Abraham D Flaxman, Robert Jakob, Jordana Leitao, Nicolas Maire, Chalapati Rao, Ian Riley, et al. The who 2016 verbal autopsy instrument: An international standard suitable for automated analysis by interva, insilicova, and tariff 2.0. *PLOS Medicine*, 15(1):e1002486, 2018.

Max Roser and Hannah Ritchie. Burden of disease. *Our World in Data*, 2018.
<https://ourworldindata.org/burden-of-disease>.

Peter Serina, Ian Riley, Andrea Stewart, Spencer L James, Abraham D Flaxman, Rafael Lozano, Bernardo Hernandez, Meghan D Mooney, Richard Luning, Robert Black, et al. Improving performance of the tariff method for assigning causes of death to verbal autopsies. *BMC medicine*, 13(1):291, 2015.

Yan D Zhao, Dewi Rahardja, De-Hui Wang, and Haili Shen. Testing homogeneity of stratum effects in stratified paired binary data. *Journal of Biopharmaceutical Statistics*, 24(3):600–607, 2014.